



## Note

# Scattering properties of heterogeneous mineral particles with absorbing inclusions



Janna M. Dlugach<sup>a</sup>, Michael I. Mishchenko<sup>b,\*</sup>

<sup>a</sup> Main Astronomical Observatory of the National Academy of Sciences of Ukraine, 27 Zabolotny Str., 03680 Kyiv, Ukraine

<sup>b</sup> NASA Goddard Institute for Space Studies, 2880 Broadway, New York, NY 10025, USA

## ARTICLE INFO

### Article history:

Received 23 December 2014

Received in revised form

20 January 2015

Accepted 22 January 2015

Available online 2 February 2015

### Keywords:

Maxwell equations

Electromagnetic scattering

Superposition *T*-matrix method

Heterogeneous particles

## ABSTRACT

We analyze the results of numerically exact computer modeling of scattering and absorption properties of randomly oriented polydisperse heterogeneous particles obtained by placing microscopic absorbing grains randomly on the surfaces of much larger spherical mineral hosts or by imbedding them randomly inside the hosts. These computations are paralleled by those for heterogeneous particles obtained by fully encapsulating fractal-like absorbing clusters in the mineral hosts. All computations are performed using the superposition *T*-matrix method. In the case of randomly distributed inclusions, the results are compared with the outcome of Lorenz–Mie computations for an external mixture of the mineral hosts and absorbing grains. We conclude that internal aggregation can affect strongly both the integral radiometric and differential scattering characteristics of the heterogeneous particle mixtures.

Published by Elsevier Ltd.

## 1. Introduction

Mineral particles are abundant in various natural and artificial environments and are often characterized using non-invasive optical techniques (see, e.g., Refs. [1–4] and references therein). Therefore, accurate numerical modeling of their scattering and absorption properties (such as the optical cross sections, single-scattering albedo, and scattering matrix) can be important in various fields of science and engineering. Quite often mineral particles have attached or imbedded absorbing impurities, which can make the calculation of their scattering and absorption properties rather involved. Whether the scattering and absorption characteristics of an external mixture of “independently scattering” mineral hosts and absorbing con-

taminants change upon aggregation depends on the strength of the resulting electromagnetic interaction between the mineral and absorbing components, which are now in direct physical contact instead of being widely separated. This interaction and the accompanying optical effects are still poorly studied and so warrant a special analysis.

Previously, in Ref. [5], we discussed potential effects caused by the adherence of small strongly absorbing grains to the surfaces of larger mineral hosts (so-called semi-external mixing [6]), as opposed to the scenario when the hosts and the grains are all widely separated (i.e., externally mixed [6]), and these effects were shown to be quite substantial. In this Note, we consider the case of internal mixing [6], wherein the absorbing grains are imbedded randomly in a larger silicate host, and compare the traits of light scattering characteristics of such heterogeneous particles with those studied in Ref. [5]. Also, we analyze the results of computations performed for a compound particle obtained by arranging the absorbing inclusions into a fractal-like cluster fully imbedded in a silicate host.

\* Corresponding author. Fax: +1 212 678 5222.

E-mail address: [michael.i.mishchenko@nasa.gov](mailto:michael.i.mishchenko@nasa.gov) (M.I. Mishchenko).

## 2. Modeling methodology

We consider three models of compound particles, each consisting of a relatively large spherical mineral host which:

- (i) is dusted by identical, small, non-overlapping, absorbing spherical grains (Model A);
- (ii) is randomly filled with identical, small, non-overlapping, absorbing spherical grains (Model B); or
- (iii) encapsulates a fractal-like cluster composed of identical, small, touching, absorbing spherical grains (Model C).

The attraction of these models consisting of only spherical components is that they allow one to isolate unequivocally the scattering effects of the host shape from the effects of the host being mixed with grains of another size and refractive index. In order to generate such scattering targets, we use random-number subroutines that create fixed quasi-random and quasi-uniform configurations of small grains while ensuring that the grains do not overlap and lie on the surface of the host or are imbedded inside the host without crossing its boundary. Fig. 1 illustrates these models of compound particles.

It is assumed that a small polydisperse group of such heterogeneous particles is illuminated by a parallel quasi-monochromatic beam of light and that the observation point is located sufficiently far from the group (e.g., Chapter 14 of Ref. [7]). It is also assumed that all scattering and absorption characteristics are averaged over the uniform orientation distribution of the resulting host–grains configurations with respect to the laboratory reference frame. The transformation of the Stokes parameters  $I$ ,  $Q$ ,  $U$ , and  $V$  caused by electromagnetic scattering by the polydisperse group of compound particles is then written in terms of the normalized Stokes scattering matrix [7,8]:

$$\begin{bmatrix} I^{\text{sca}} \\ Q^{\text{sca}} \\ U^{\text{sca}} \\ V^{\text{sca}} \end{bmatrix} \propto \begin{bmatrix} a_1(\theta) & b_1(\theta) & 0 & 0 \\ b_1(\theta) & a_2(\theta) & 0 & 0 \\ 0 & 0 & a_3(\theta) & b_2(\theta) \\ 0 & 0 & -b_2(\theta) & a_4(\theta) \end{bmatrix} \begin{bmatrix} I^{\text{inc}} \\ Q^{\text{inc}} \\ U^{\text{inc}} \\ V^{\text{inc}} \end{bmatrix}, \quad (1)$$

where  $\theta \in [0^\circ, 180^\circ]$  is the angle between the incidence (“inc”) and scattering (“sca”) directions, while both Stokes column vectors are defined with respect to the scattering plane. In our notation, the zeros denote the scattering

matrix elements negligibly small (in the absolute-value sense) relative to the nonzero elements at the same scattering angles. The (1,1) element,  $a_1(\theta)$ , is called the phase function and satisfies the integral normalization condition

$$\frac{1}{2} \int_0^\pi a_1(\theta) \sin \theta d\theta = 1. \quad (2)$$

The elements of the scattering matrix (1) can be used to identify specific optical observables corresponding to different types of polarization state of the incident radiation. For example, if the incident beam is unpolarized then the phase function characterizes the angular distribution of the scattered intensity, while the ratio  $-b_1/a_1$  gives the degree of linear polarization of the scattered light. In the case of linearly polarized incident light, the ratio  $a_2/a_1$  can serve as an indicator of nonsphericity of the scattering particles (e.g., [7,8]).

The specific morphologies of the three models of compound aerosols allow us to compute all their scattering and absorption characteristics using the highly efficient and numerically exact superposition  $T$ -matrix method [9,10] implemented in the form of the public-domain parallelized FORTRAN program MSTM Version 3.0 [11]. To eliminate oscillations typical of monodisperse particles [7,8], we average all scattering and absorption characteristics over a standard power-law size distribution

$$n(R) = \begin{cases} \text{constant} \times R^{-3}, & R_1 \leq R \leq R_2, \\ 0, & \text{otherwise.} \end{cases} \quad (3)$$

Another benefit of size averaging is that it yields a better quantitative representation of polydisperse particle ensembles typically encountered in natural and artificial environments.

## 3. Numerical modeling and discussion

### 3.1. Mixtures of host particles with randomly distributed small grains

In order to identify distinct optical effects of absorbing grains randomly imbedded in mineral hosts, all computations were performed for the same parameter values as in Ref. [5]. Specifically, the ratio of the radius of a mineral host to that of small absorbing grains was kept constant at  $R/r \equiv 10$ . The numerical size averaging according to

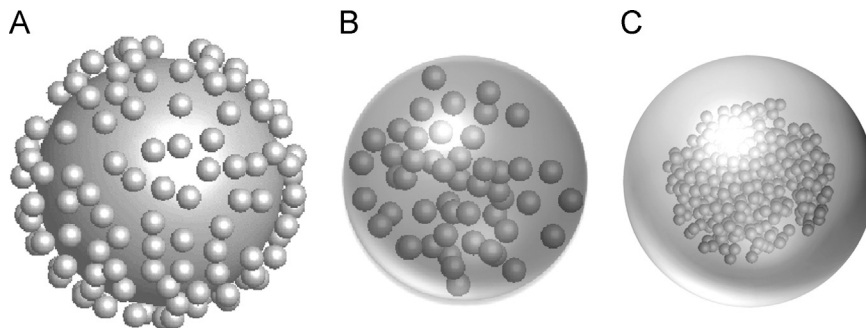


Fig. 1. Three models of compound particles.

Eq. (3) was based on the Gauss–Legendre integration quadrature formula with 100 nodes in the range  $0.661 \mu\text{m} \leq R \leq 1.439 \mu\text{m}$ , corresponding to an effective radius of the mineral hosts  $R_{\text{eff}}=1 \mu\text{m}$ , the effective radius of the absorbing grains  $r_{\text{eff}}=0.1 \mu\text{m}$ , and the effective variance of the size distribution  $v_{\text{eff}}=0.05$ . The refractive indices of the mineral hosts and absorbing grains were adopted to be  $1.55+i0.0003$  and  $1.75+i0.435$ , respectively, while the wavelength  $\lambda$  was fixed at  $0.6283 \mu\text{m}$ . Here, we discuss the results of computations performed assuming that the number of absorbing grains per mineral host is  $N_g=49$  or  $149$ .

Table 1 lists the resulting ensemble-averaged integral radiometric characteristics, viz., the extinction,  $C_{\text{ext}}$ , scattering,  $C_{\text{sca}}$ , and absorption,  $C_{\text{abs}}$ , cross sections as well as the single-scattering albedo  $\omega$  and the asymmetry parameter  $g$ .

**Table 1**  
Polydisperse mineral hosts with randomly distributed absorbing grains. Ensemble-averaged extinction, scattering, and absorption cross sections (in  $\mu\text{m}^2$ ) per compound particle “host+ $N_g$  grains”, single-scattering albedo  $\omega$ , and asymmetry parameter  $g$ .

$N_g$	$C_{\text{ext}}$	$C_{\text{sca}}$	$C_{\text{abs}}$	$\omega$	$g$
0 (pure host)	6.314	6.265	0.049	0.9923	0.668
49 <sub>ind</sub>	8.279	6.924	1.355	0.836	0.635
149 <sub>ind</sub>	12.291	8.268	4.023	0.673	0.585
49 <sub>A</sub>	6.925	5.678	1.247	0.820	0.730
149 <sub>A</sub>	7.832	5.161	2.671	0.659	0.819
49 <sub>B</sub>	6.596	4.599	1.997	0.697	0.773
149 <sub>B</sub>	7.168	3.845	3.323	0.536	0.878

The subscripts in the left-most column specify the distribution of  $N_g$  absorbing grains relative to the mineral host: the subscript “ind” denotes a uniform external mixture of the mineral hosts and absorbing grains resulting in “independently scattering” components; the subscript “A” applies to the case of absorbing grains randomly covering the surfaces of the mineral hosts, i.e., Model A; and the subscript “B” denotes the case of encapsulated, randomly distributed absorbing grains, i.e., Model B. The data in the first five rows of Table 1 were taken from Ref. [5].

One can see that:

- (i) The presence and increasing number  $N_g$  of absorbing grains always increases the extinction and absorption cross sections; the increase in the extinction cross sections is slower in the case of Model B, while the slowest increase in the absorption cross section is observed for Model A.
- (ii) The presence and increasing number  $N_g$  of absorbing grains always decreases the single-scattering albedo  $\omega$ . This can be explained by the suppression of the contribution of the weakly absorbing mineral hosts to the total scattered light, the suppression being more pronounced for Model B.
- (iii) The asymmetry parameter  $g$  in the external-mixture case decreases with increasing  $N_g$  because the asymmetry parameter of the small absorbing grains is much smaller than that of the large mineral hosts. In the case of Models A and B, increasing  $N_g$  causes the resulting phase function to be increasingly controlled by the forward-scattering diffraction peak and thereby to become progressively anisotropic.

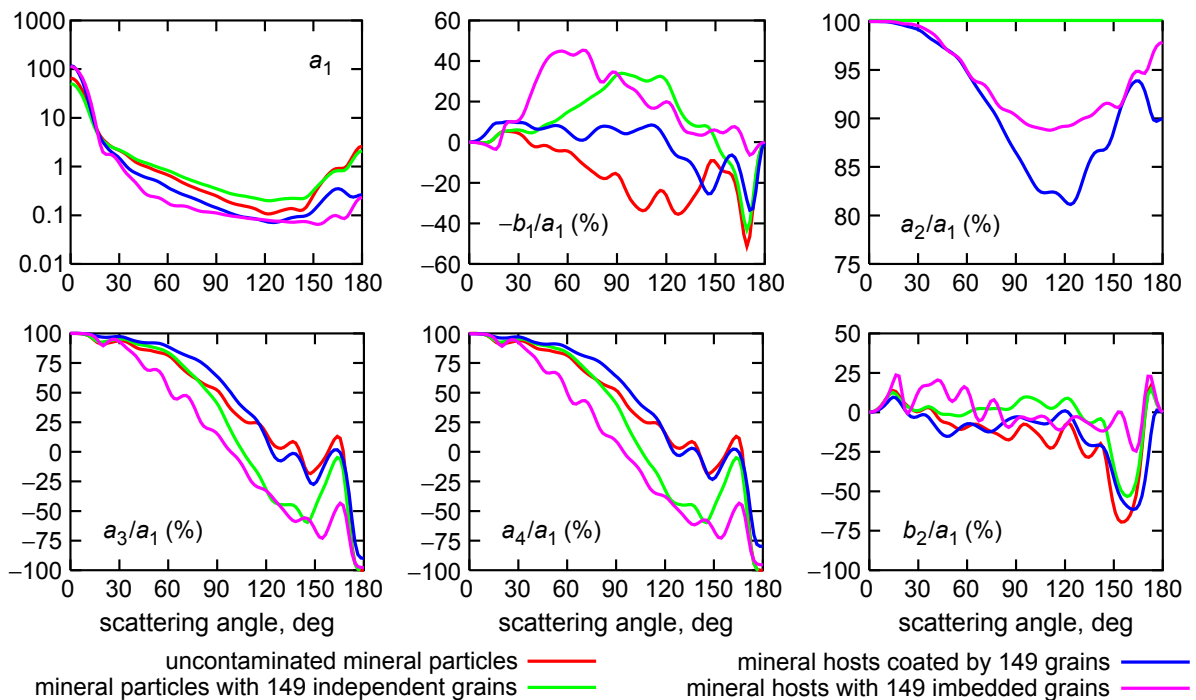


**Fig. 2.** Elements of the normalized Stokes scattering matrix for uncontaminated mineral particles as well as for different types of mixture of a mineral host with  $N_g=149$  absorbing grains. (For interpretation of the references to color in this figure, the reader is referred to the web version of this article.)

Fig. 2 visualizes the dependence of all non-zero elements of the normalized Stokes scattering matrix (1) on the type of compound aerosol. Here, for the case of  $N_g=149$ , we depict the results of computations performed for the external mixture of mineral particles and absorbing grains (green curves), mineral hosts coated by absorbing grains (blue curves), and mineral hosts with encapsulated absorbing grains (pink curves). For comparison, we also plot the data corresponding to uncontaminated mineral particles (red curves).

The upper left-hand panel demonstrates a strong effect of aggregation on the phase function, especially in the case of encapsulated absorbing grains. The phase functions show order-of-magnitude differences at backscattering angles and pronounced differences at side-scattering angles. Interestingly, however, at the exact backscattering direction the phase-function values for Models A and B are essentially the same.

The upper middle panel also illustrates a potentially strong effect of the type of particle heterogeneity on the degree of linear polarization. In particular, the polarization becomes more neutral at side-scattering angles when absorbing grains cover the surfaces of mineral hosts, whereas it is substantially positive in the external-mixing case as well as in the case of encapsulated absorbing grains. At backscattering angles, a deep negative minimum occurs for all particle types except for Model B.

The ratio  $a_2/a_1$  (see the upper right-hand panel) is identically equal to 100% for uncontaminated mineral hosts and for the external mixture of mineral hosts and absorbing grains, but deviates from 100% for Models A and B, thereby revealing the most symptomatic trait of compound particles lacking perfect spherical symmetry. The

presence of encapsulated absorbing grains results in a somewhat smaller deviation from 100% compared to the case of absorbing grains covering the surfaces of the mineral hosts. This may qualitatively be explained by the stronger effect of the spherical surface of the mineral hosts in the case of Model B.

The data depicted in the bottom panels also reveal noticeable effects caused by different types of aggregation on the ratios  $a_3/a_1$ ,  $a_4/a_1$ , and  $b_2/a_1$ , especially in the case of Model B.

Fig. 3 demonstrates the effects of increasing the number of absorbing grains on the behavior of the elements of the Stokes scattering matrix for compound particles. It shows the numerical results for  $N_g=49$  and 149 absorbing grains covering the surfaces of or being randomly imbedded inside mineral hosts. It is seen that for both types of aggregation the phase function  $a_1$  and the degree of linear polarization  $-b_1/a_1$  change significantly with  $N_g$  and that for Model B this effect is much more pronounced. However, the curves in the bottom panels show a strong dependence on  $N_g$  of the ratios  $a_3/a_1$ ,  $a_4/a_1$ , and  $b_2/a_1$  only for Model B.

### 3.2. Absorbing fractal clusters imbedded in spherical mineral hosts

It is well known that tropospheric soot aerosols often exist in the form of clusters consisting of large numbers of monomers. Extensive analyses of scattering properties of such particles based on the results of numerically exact solutions of the Maxwell equations have been performed in, e.g., Refs. [12–16] (see also the reference list in Ref. [17]). In particular, the case when a larger dust particle

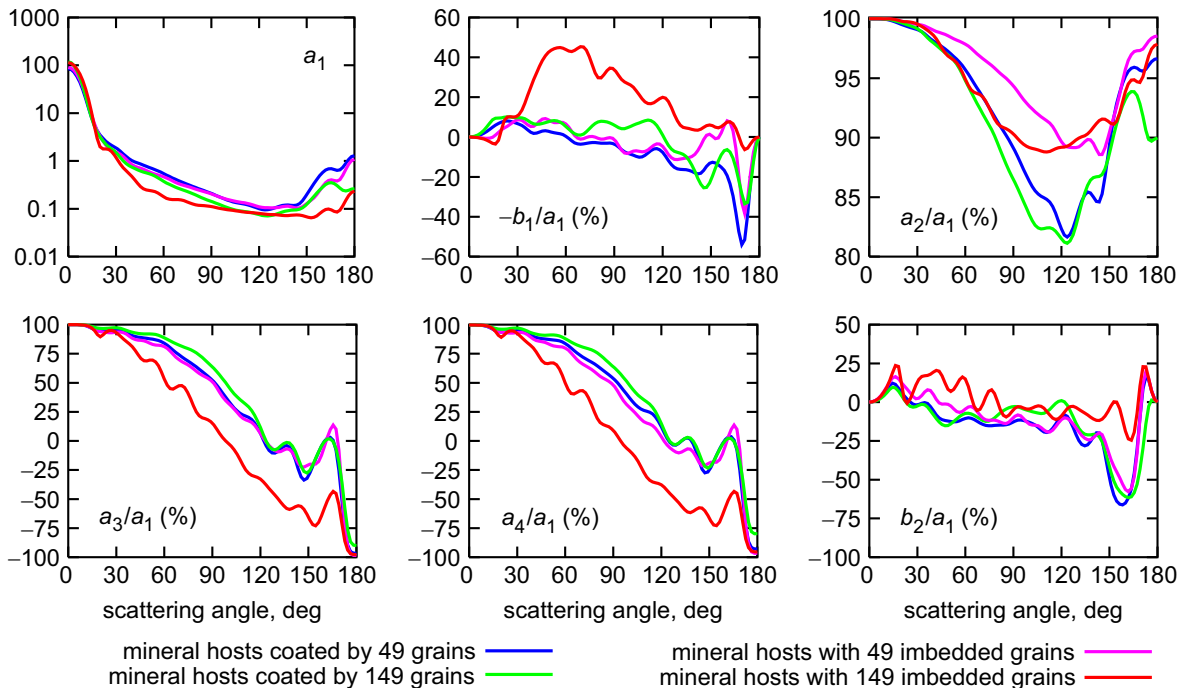


Fig. 3. As in Fig. 2, but for composite particles with  $N_g=49$  and 149 absorbing grains.

touches a soot cluster was studied in Ref. [13], while Ref. [16] described an analysis of optical properties of compound particles consisting of an internal mixture of cloud water droplets with black-carbon fractal clusters. A thorough analysis of the optical properties of heterogeneous aerosols composed of soot clusters imbedded in sulfate particles was performed in Ref. [15]. To parallel the analyses in Refs. [15,16], we consider polydisperse heterogeneous particles obtained by imbedding an absorbing fractal cluster inside a spherical mineral host.

We assume that the absorbing fractal cluster is composed of identical spherical monomers and parameterize its morphology by the standard statistical-scaling law [18]

$$N_s = k_0 \left( \frac{R_g}{r} \right)^{D_f}, \quad (4)$$

where  $r$  is the monomer radius,  $1 \leq D_f \leq 3$  is the fractal dimension,  $k_0$  is the fractal prefactor,  $N_s$  is the number of

**Table 2**

Polydisperse mineral hosts with encapsulated fractal clusters of absorbing grains. Ensemble-averaged extinction, scattering, and absorption cross sections (in  $\mu\text{m}^2$ ) per compound particle “host+cluster”, single-scattering albedo  $\omega$ , and asymmetry parameter  $g$ .

Model	$C_{\text{ext}}$	$C_{\text{sca}}$	$C_{\text{abs}}$	$\omega$	$g$
1	0.933	0.931	0.002	0.9987	0.706
2	0.891	0.783	0.108	0.878	0.697
3	2.379	2.372	0.007	0.9974	0.641
4	2.162	1.728	0.434	0.799	0.699

monomers in the cluster, and  $R_g$  is the radius of gyration serving as a measure of the overall cluster radius. We again consider polydisperse compound particles, with two values of the effective radius of the mineral hosts  $R_{\text{eff}}=0.3 \mu\text{m}$  (corresponding to the size range  $0.219 \mu\text{m} \leq R \leq 0.399 \mu\text{m}$ ) and  $R_{\text{eff}}=0.5 \mu\text{m}$  (with  $0.365 \mu\text{m} \leq R \leq 0.665 \mu\text{m}$ ). These size ranges imply the same effective-variance value  $\nu_{\text{eff}}=0.03$ . We further adopt the fractal parameters  $D_f=2.6$  and  $k_0=1.2$ , while fixing the effective radius of the absorbing monomers at  $r_{\text{eff}}=0.025 \mu\text{m}$  and the wavelength at  $\lambda=0.6283 \mu\text{m}$ . The volume fraction of a cluster in a compound particle  $f$  is fixed at 6.25%, which implies that  $N_s=108$  for  $R_{\text{eff}}=0.3 \mu\text{m}$  and  $N_s=500$  for  $R_{\text{eff}}=0.5 \mu\text{m}$ . Computations were performed for the following four models: uncontaminated polydisperse mineral hosts with  $R_{\text{eff}}=0.3 \mu\text{m}$  (Model 1); polydisperse mineral hosts with  $R_{\text{eff}}=0.3 \mu\text{m}$  with imbedded clusters composed of  $N_s=108$  absorbing monomers (Model 2); as in Model 1, but with  $R_{\text{eff}}=0.5 \mu\text{m}$  (Model 3); and as in Model 2, but with  $R_{\text{eff}}=0.5 \mu\text{m}$  and  $N_s=500$  (Model 4).

Table 2 summarizes the corresponding ensemble-averaged integral radiometric characteristics. For both values of  $R_{\text{eff}}$ , the insertion of an absorbing cluster inside a mineral host results in a noticeable decrease in the extinction and scattering cross sections and a dramatic increase in the absorption cross section, the latter causing a decrease in the single-scattering albedo. This tendency is more pronounced for  $R_{\text{eff}}=0.5 \mu\text{m}$ . On the other hand, the behavior of the asymmetry parameter depends on the size of the mineral hosts. Specifically,  $g$  slightly decreases

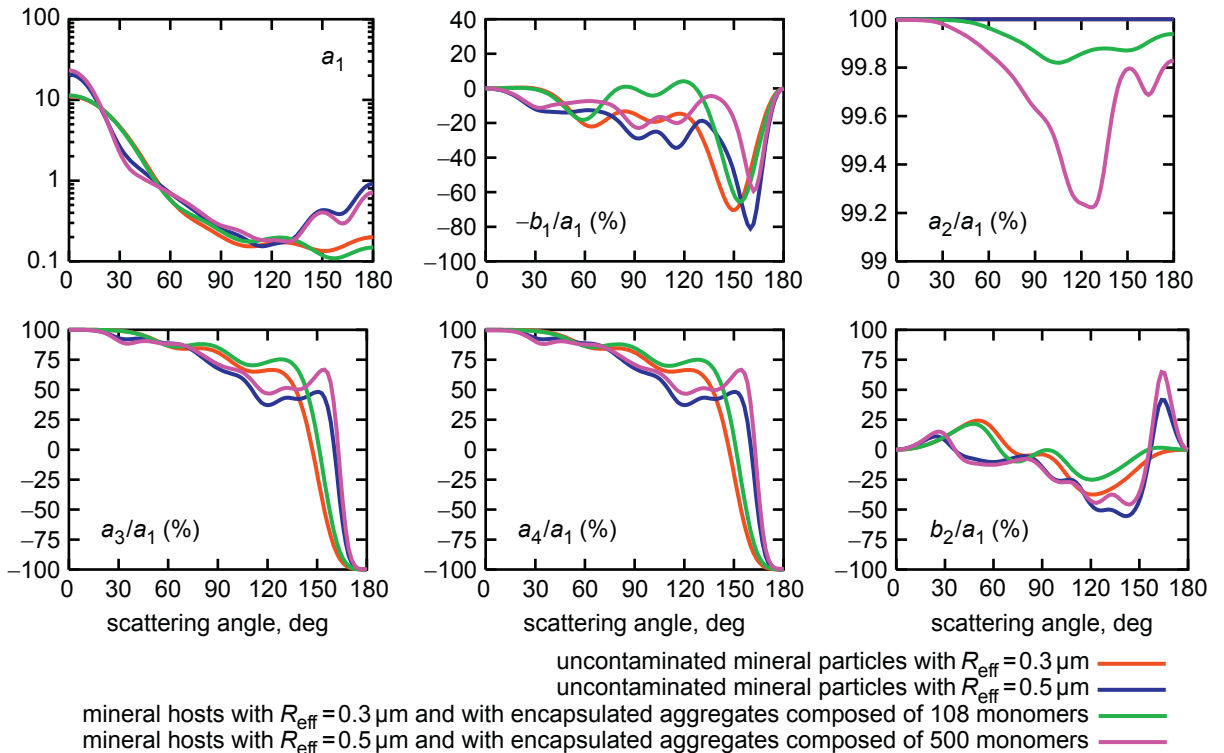


**Fig. 4.** As in Fig. 2, but for uncontaminated mineral particles with  $R_{\text{eff}}=0.3$  and  $0.5 \mu\text{m}$  as well as for mineral hosts with  $R_{\text{eff}}=0.3$  and  $0.5 \mu\text{m}$  each encapsulating a fractal-like cluster composed of  $N_s=108$  and 500 absorbing grains, respectively.

in the case of the smaller hosts with  $R_{\text{eff}}=0.3 \mu\text{m}$ , but increases in the case of  $R_{\text{eff}}=0.5 \mu\text{m}$ .

In Fig. 4, we plot the corresponding non-zero elements of the normalized Stokes scattering matrix. It is seen that for both host sizes, the optical effects of inserting absorbing clusters are rather weak. In particular, the phase function slightly decreases at backscattering angles; the degree of linear polarization  $-b_2/a_1$  becomes more neutral at side-scattering angles (especially for  $R_{\text{eff}}=0.3 \mu\text{m}$ ); and the ratio  $a_2/a_1$  deviates slightly from 100% (especially for  $R_{\text{eff}}=0.5 \mu\text{m}$ ), thereby indicating the loss of spherical symmetry in compound particles. It is quite possible that these rather insignificant changes can be explained by the relatively small value of the cluster volume fraction ( $f=6.25\%$ ) and can become greater for larger  $f$ .

#### 4. Concluding remarks

Our numerically exact computer solutions of the Maxwell equations demonstrate that optical effects caused by contaminating mineral particles with absorbing inclusions can often be significant. Specifically, all integral radiometric characteristics can change quite substantially, especially in the case of internally mixed absorbing grains. Furthermore, there is strong sensitivity of some integral and differential optical properties to the type of mixing and/or to the total volume fraction of the impurities. In particular, the phase function  $a_1$  can exhibit an order-of-magnitude variability at backscattering angles and significant changes at side-scattering angles, while the degree of linear polarization  $-b_1/a_1$  becomes more neutral at side-scattering angles when absorbing grains cover the surfaces of the mineral hosts but is positive if the absorbing grains are mixed internally. On the other hand, strong variations in the ratios  $a_3/a_1$ ,  $a_4/a_1$ , and  $b_2/a_1$  with increasing the number of absorbing grains  $N_g$  are observed only in the case of internal mixing. The ratio  $a_2/a_1$  (which is indicative of the lack of perfect spherical symmetry in the particle morphology) appears to depend noticeably on type of aggregation (internal or semi-external) but rather weakly on the number of absorbing grains  $N_g$ . Our data show rather weak effects of the presence of imbedded absorbing clusters on the elements of the scattering matrix. However, this conclusion may need to be revised when larger volume fractions occupied by the clusters are considered.

We hope that the results of this Note will be useful in optical particle characterization applications as well as in radiation budget computations.

#### Acknowledgments

We thank Alexandra Ivanova for help with Fig. 1. JMD acknowledges support from the National Academy of

Sciences of Ukraine under the Main Astronomical Observatory GRAPE/GPU/GRID Computing Cluster Project. She also thanks the organizers of the LIP 2014 conference for providing full financial support. MIM was supported by the NASA Radiation Sciences Program and the NASA ACE Project managed by Hal Maring as well as by the NASA Remote Sensing Theory Program managed by Lucia Tsaoussi.

#### References

- [1] Davis EJ, Schweiger G. The airborne microparticle. Heidelberg: Springer; 2002.
- [2] Li J, Anderson JR, Buseck PR. TEM study of aerosol particles from clean and polluted marine boundary layers over the North Atlantic. J Geophys Res 2003;108:4189.
- [3] Reid EA, Reid JS, Meier MM, et al. Characterization of African dust transported to Puerto Rico by individual particle and size segregated bulk analysis. J Geophys Res 2003;108:8591.
- [4] Kulkarni P, Baron PA, Willeke K, editors. Aerosol measurement: principles, techniques, and applications. New York: Wiley; 2011.
- [5] Mishchenko MI, Dlugach JM. Adhesion of mineral and soot aerosols can strongly affect their scattering and absorption properties. Opt Lett 2012;37:704–6.
- [6] Mishchenko MI, Liu L, Travis LD, Lacis AA. Scattering and radiative properties of semi-external versus external mixtures of different aerosol types. J Quant Spectrosc Radiat Transf 2004;88:139–47.
- [7] Mishchenko MI. Electromagnetic scattering by particles and particle groups: an introduction. Cambridge: Cambridge University Press; 2014.
- [8] Mishchenko MI, Travis LD, Lacis AA. Scattering, absorption, and emission of light by small particles. Cambridge: Cambridge University Press; 2002. (<http://www.giss.nasa.gov/staff/mmishchenko/books.html>).
- [9] Mackowski DW, Mishchenko MI. Calculation of the  $T$  matrix and the scattering matrix for ensembles of spheres. J Opt Soc Am A 1996;13:2266–78.
- [10] Mackowski DW, Mishchenko MI. A multiple sphere  $T$ -matrix Fortran code for use on parallel computer clusters. J Quant Spectrosc Radiat Transf 2011;112:2182–92.
- [11] Mackowski DW. (<http://www.eng.auburn.edu/users/dmckowski/scatcodes>).
- [12] Liu L, Mishchenko MI. Effects of aggregation on scattering and radiative properties of soot aerosols. J Geophys Res 2005;110:D11211.
- [13] Liu L, Mishchenko MI. Scattering and radiative properties of complex soot and soot-containing aggregate particles. J Quant Spectrosc Radiat Transf 2007;106:262–73.
- [14] Liu L, Mishchenko MI, Arnott WP. A study of radiative properties of fractal soot aggregates using the superposition  $T$ -matrix method. J Quant Spectrosc Radiat Transf 2008;109:2656–63.
- [15] Kahnert M, Nousiainen T, Lindqvist H. Models for integrated and differential scattering optical properties of encapsulated light absorbing carbon aggregates. Opt Express 2013;21:7974–93.
- [16] Mishchenko MI, Liu L, Cairns B, Mackowski DW. Optics of water cloud droplets mixed with black-carbon aerosols. Opt Lett 2014;39:2607–10.
- [17] Mishchenko MI, Liu L, Mackowski DW.  $T$ -matrix modeling of linear depolarization by morphologically complex soot and soot-containing aerosols. J Quant Spectrosc Radiat Transf 2013;123:135–44.
- [18] Sorensen CM. Light scattering by fractal aggregates: a review. Aerosol Sci Technol 2001;35:648–87.